Desalination and Water Treatment
www.deswater.com
1944-3994/1944-3986 © 2013 Desalination Publications. All rights reserved
doi: 10.1080/19443994.2012.694238

51 (2013) 374–383
January

Taylor & Francis
Taylor & Francis Group

Oxidation–microfiltration removal of Fe(II) from water

Lanny Setyadhi, J.C. Liu*

Department of Chemical Engineering, National Taiwan University of Science and Technology, 43 Keelung Road, Section 4, Taipei 106, Taiwan
Tel. +886 2 2737 6627; Fax: +886 2 2737 6644; email: liu1958@mail.ntust.edu.tw

Received 28 February 2012; Accepted 10 May 2012

ABSTRACT

We studied iron removal from water by oxidation and microfiltration. Water sample containing ferrous ion was oxidized by air at a constant flow rate and pH. The suspension was then subjected to crossflow microfiltration using mixed cellulose ester and polyvinylidene fluoride membranes. Results reveal that iron removal efficiency mainly depended on oxidation process conditions, and the filtration process enhanced iron removal efficiency. Oxidation process at pH 8 followed by microfiltration produced permeate containing iron at concentrations below 0.3 mg/L, while a slightly higher iron concentration was found at pH 7.5. Under laminar and turbulent flow conditions, permeate flux increased as the filtration pressure varied from 5 to 10 psi. Increasing crossflow velocity from 0.48 to 1.33 m/s increased the permeate flux. Cake resistance was the dominant resistance causing decline in flux under all filtration conditions. Cake resistance increased with filtration pressure and decreased with the increase in crossflow velocity. The presence of Mn(II) and humic acids (HA) decreased iron removal efficiency and permeate flux. Permeate flux increased with initial Mn(II) concentrations and decreased with increasing HA concentration.

Keywords: Humic acids; Iron; Manganese; Microfiltration; Oxidation; Water

1. Introduction

Iron is one of the common metallic elements found in the earth's crust, and it is the essential element for humans, plants, and animals [5]. Iron itself is relatively harmless to health, but it may increase the hazard of pathogenic organisms, since many of them need Fe to grow [5]. Iron (Fe) and manganese (Mn) cause some certain problems because of metallic taste, odor, stains in cloths, interference during treatment process, and formation of deposits in distribution systems [5,25].

The maximum recommended levels of Fe and Mn concentrations for drinking water are 0.2 and 0.05 mg/L, respectively, in the European Communities Drinking Water Regulations 2007 [8]; 0.3 and 0.1 mg/L in the Guidelines for Drinking Water Quality by World Health Organization [31]; 0.3 and 0.05 mg/L in the National Secondary Drinking Water Regulations by US EPA and in the Guidelines for Taiwanese Drinking Water Quality.

There are many physico-chemical methods to remove Fe and Mn. High-pressure membrane filtration (nanofiltration and reverse osmosis) can be

*Corresponding author.

Presented at the International Conference on Desalination for the Environment, Clean Water and Energy, European Desalination Society, 23–26 April 2012, Barcelona, Spain

applied to remove metals from waters [3,25]. Softening and sand filter processes are effective for water containing lower contaminants at lower concentrations [3,7]. Adsorption can remove metals in the presence of organic matter. However, it has critical problems related to the regeneration and disposal of spent adsorbents [2]. Oxidation using oxidants, such as oxygen, air, potassium permanganate, ozone, chlorine, chlorine dioxide, and hydrogen peroxide is feasible. Ferrous iron, Fe(II), is easily oxidized when it comes into contact with air. Ferric iron, Fe(III), then forms iron oxides or iron hydroxide precipitates [12,13,21]. Iron oxides consist of oxides, hydroxides, and oxyhydroxides [10,24]. The reaction mechanism of iron oxidation is as follows [13,26]:

$$\text{Oxidation} \quad 4Fe^{2+}O_2 + 4H^+ \leftrightarrow 4Fe^{2+} + 2H_2O$$

$$\text{Hydrolysis} \quad \frac{Fe^{3+} + 3H_2O \leftrightarrow Fe(OH)_3 + 3H^+ \quad (x4)}{4Fe^{2+} + 10H_2O + O_2 \rightarrow 4Fe(OH)_3 + 8H^+}$$

Microfiltration offers several advantages, including better water quality by removing colloids and pathogens, lower maintenance, and lesser sludge production [17,20]. The driving force for water transport across the microporous membrane is the pressure gradient across the membrane, namely trans-membrane pressure. Crossflow filtration is a good technique to minimize particle deposition and membrane fouling by maintaining a high scour velocity on the membrane surface. Permeate flux is limited by the layer of particles deposited on the membrane, called dynamic membrane [15,29].

This study investigates Fe(II) removal efficiency using oxidation by air, followed by crossflow microfiltration. Various operating conditions, such as membrane types, filtration pressure, and crossflow velocity, are examined. The effects of Mn(II) and humic acids (HA) on Fe removal efficiency are also investigated.

2. Materials and methods

Synthetic water sample was made by dissolving a fixed amount of ferrous sulfate hepta-hydrate ($FeSO_4 \cdot 7H_2O$) in de-ionized water in a 1,000-mL volumetric flask. The pH of the water sample was adjusted to the desired pH (±0.1) with 0.1 N NaOH or 0.1 N HCl and the initial turbidity and Fe concentration were measured. It was then oxidized by air under slow mixing (30 rpm) at a constant contact time and air flowrate. The optimum pH found was used in further experiments. The oxidized water sample or the suspension was analyzed for turbidity, total suspended solids (TSS), and Fe concentration using atomic absorption spectrometer (Varian, SpectrAA-20). Manganese concentration was analyzed by atomic absorption spectrometer, while HA concentration was represented by the total organic carbon analyzed by an analyzer (Tekmar Dohrmann, Phoenix 8000). The iron oxide was characterized by X-ray diffraction (Rigaku, D/MAX-RC), field emission scanning electron microscope (JEOL, JSM-6500F), zeta meter (Malvern, Zetasizer 2000), and particle sizer (Malvern, Mastersizer 2000).

The suspension was stirred in a tank to ensure that there are no solids settled in the tank. The use of crossflow microfiltration apparatus can be found in our previous work [14]. Each filtration experiment was conducted for 3 h. The temperature of the suspension was maintained at 25°C to eliminate the effects of temperature. This procedure was repeated with different membrane types (mixed cellulose ester hydrophilic membrane and polyvinylidene fluoride [PVDF] hydrophobic membrane), filtration pressures (5, 8, and 10 psi), and crossflow velocities (0.48, 0.90, and 1.33 m/s). The filtrate was then analyzed for iron concentration. The cake on the membrane was collected and weighed. The suspension in the tank was analyzed for TSS and particle size distribution. Mixed cellulose ester and PVDF were immersed in water and alcohol, respectively, to ensure maximum wettability.

3. Results and discussion

3.1. Oxidation and microfiltration

X-ray analysis revealed that lepidocrocite was produced by the oxidation process at pH 7.5, and at pH 8 the formation of lepidocrocite along with magnetite was favored. Isoelectric point (pH_{IEP}) of iron oxide precipitates was found at pH 7.8, which is approximately equal to reported values of lepidocrocite at pH 5.4–7.4 and of magnetite at pH 6.5 and 8 [23]. The difference in the surface charge of iron oxides produced by oxidation at pH 7.5 and 8 was insignificant. Fig. 1 (A) shows decline in flux under various pH when using hydrophilic (mixed cellulose ester) membrane at 5 psi. The initial flux was 1,335 and 1,080 L/m^{2}h, respectively, at pH 7.5 and 8. The flux decreased until steady-state flux was reached. The steady flux was 350 and 245 L/m^{2}h, respectively, at pH 7.5 and 8. It showed that both the initial and steady fluxes at pH 7.5 were higher than those at pH 8 because of the higher iron oxidation rate and the higher amount of iron oxides formed at higher pH [1]. The opposite phenomena occurred at a higher filtration pressure of

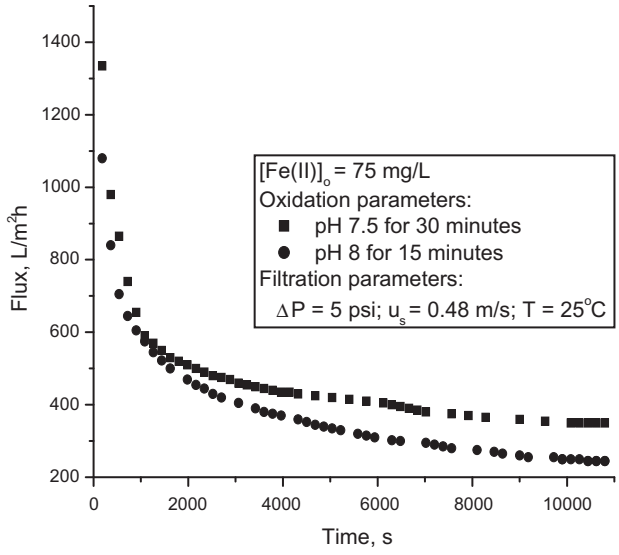

Fig. 1A. Effects of oxidation condition on flux using hydrophilic (mixed cellulose ester) membrane at 5 psi.

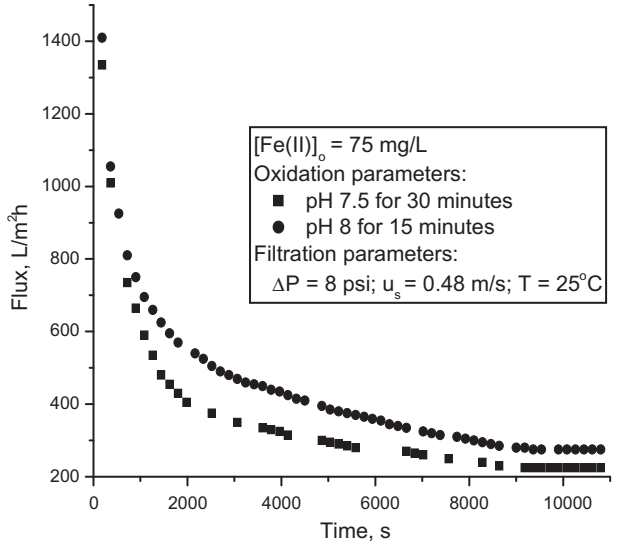

Fig. 1B. Effects of oxidation condition on flux using hydrophilic (mixed cellulose ester) membrane at 8 psi.

8 psi (Fig. 1(B)). The initial flux was 1,335 and 1,410 L/m^2h, respectively, for filtration at pH 7.5 and 8. The steady flux was 225 and 275 L/m^2h, respectively, for filtration at pH 7.5 and 8. The initial and steady fluxes at pH 8 were higher than those at pH 7.5. It might be due to the larger size of iron particles at pH 8 (Table 1), which were easier to remove in crossflow membrane filtration.

Fe removal efficiency at pH 8 was higher than that at pH 7.5 (Table 1). The combination of oxidation and microfiltration processes resulted in higher Fe removal efficiency than the combination of oxidation and sedimentation processes. The concentrations of Fe after oxidation followed by the sedimentation process, either at pH 7.5 or 8, were higher than the guideline. The higher residual turbidity also revealed that the sedimentation process could not separate iron oxides from water as effectively as the filtration process. The turbidity of the suspension after oxidation followed by the sedimentation process at pH 7.5 was higher than that at pH 8. The higher turbidity at pH 7.5 was related to the smaller size of iron oxide particles, which had difficulty to settle. Iron oxides have a small size at a low pH and a larger size at a high pH [13]. Iron oxide particles became larger after microfiltration (Table 1). Further oxidation in the filtration system produced metal oxides/hydroxides as a result of adsorption or co-precipitation rather than the precipitation process [12].

Fig. 2(A) shows decline in flux under two different pH conditions while using hydrophobic (PVDF) membrane at 5 psi. The initial flux was 1,040 and 955 L/m^2h, and the steady flux was 365 and 280 L/m^2h at pH 7.5 and 8, respectively. The initial and steady fluxes of the filtration process using hydrophobic (PVDF) membrane were higher at pH 7.5 than those at pH 8. It is in agreement with the results obtained using hydrophilic membrane. However, the steady flux obtained by filtration using hydrophilic membrane was lower than that using hydrophobic membrane. It was likely that iron oxides are hydrophilic and tend to attach more strongly to the hydrophilic membrane surface. The stronger attachment of iron oxides to the hydrophilic membrane surface would result in higher resistances and lower steady state flux.

Fig. 2(B) shows flux at pH 7.5 and 8.0 while using hydrophobic (PVDF) membrane at 8 psi. The initial flux was 1,365 and 1,400 L/m^2h, respectively, at pH 7.5 and 8. The steady flux was 250 and 315 L/m^2h, respectively, at pH 7.5 and 8. The initial and steady fluxes at pH 8 were higher than those at pH 7.5, which were consistent with the result obtained by filtration using hydrophilic membrane. Table 2 shows that the removal efficiency of the sedimentation process was not as high as that of the microfiltration process. Oxidation followed by sedimentation processes produced water with Fe concentrations higher than the guideline. Almost all the results obtained by microfiltration using hydrophobic membrane were similar to those using hydrophilic membrane, as shown in Tables 1 and 2. It is noted that at pH 7.5, the Fe concentration in permeate was higher than the guideline. The performance of the membrane filtration process depends on particle size, and particles larger

Table 1
Residual Fe concentration and turbidity under different oxidation conditions using hydrophilic (mixed cellulose ester) membrane as compared to sedimentation

pH	Conditions	Residual Fe (mg/L)	Residual turbidity (NTU)	Median diameter (μm)
7.5 (5 psi)	Sedimentation	3.19	3.77	0.62
	Microfiltration	0.25	0.00	0.72
8 (5 psi)	Sedimentation	1.85	1.04	0.86
	Microfiltration	0.08	0.00	1.29
7.5 (8 psi)	Sedimentation	3.30	3.81	0.66
	Microfiltration	0.25	0.00	1.00
8 (8 psi)	Sedimentation	1.85	1.04	0.87
	Microfiltration	0.09	0.00	2.97

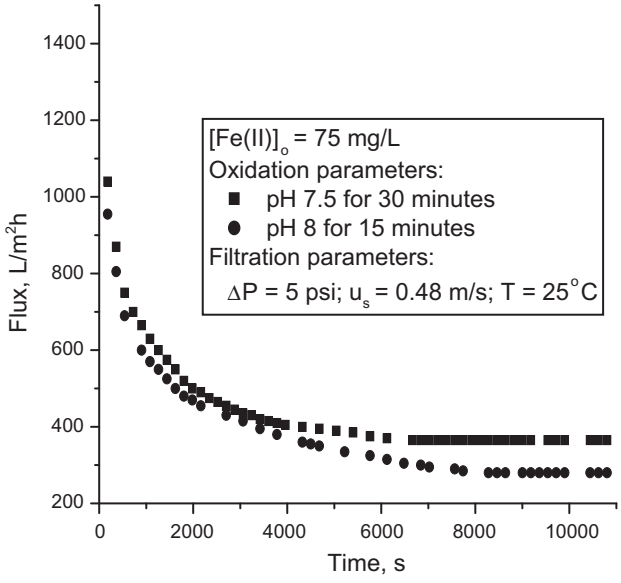

Fig. 2A. Effects of oxidation condition on flux using hydrophobic (PVDF) membrane at 5 psi.

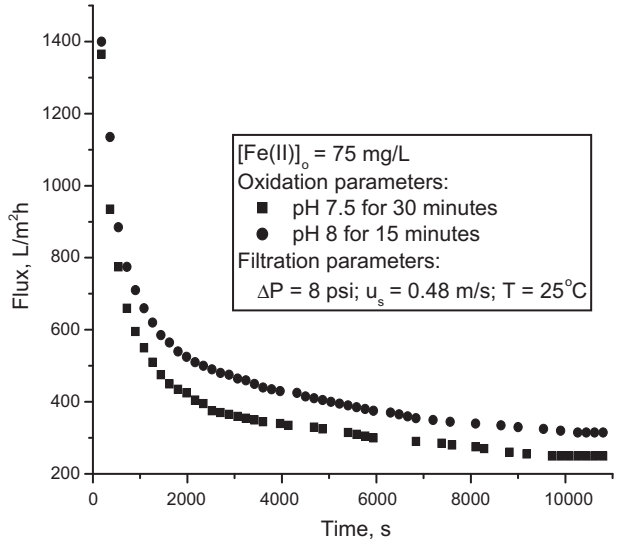

Fig. 2B. Effects of oxidation condition on flux using hydrophobic (PVDF) membrane at 8 psi.

than the membrane pore will be rejected. The size of iron oxides after the oxidation process was similar (Tables 1 and 2). The similarity of particle size should result in similar removal efficiency or rejection, but it was not found in this experiment. The lower removal efficiency of the filtration process using hydrophobic membrane might be related to hydrophobic interaction. As mentioned previously, iron oxides tended to attach strongly to the hydrophilic membrane surface. The particles deposited on the membrane surface act as pre-coated filter or secondary membrane [16,29].

3.2. Effects of filtration pressure and crossflow velocity

The resistance to filtration was analyzed using equations that divide total resistance (R_t) into resistance of the clean membrane (R_m), resistance of fouling (R_f), and resistance of cake (R_c) [17,29]. In addition, the relationship between cake resistance, cake mass per unit filtration area (w_c), and specific cake resistance (α_{av}) can be assessed [17]. Table 3 shows that cake resistance contributed more than 50% of total resistance regardless of pH, membrane types, and filtration pressure. The cake resistance increased with increasing filtration pressure because the higher filtration pressure resulted in higher cake compressibility, higher cake mass on the membrane surface, and higher cake resistance [15,16]. The higher cake resistance was observed while using hydrophilic membrane than that using hydrophobic membrane for the filtration process because of the hydrophilic interaction between the iron oxides and the membrane surface. Membrane resistance (R_m) might vary with filtration pressure, as shown in Table 3. However, it

Table 2
Residual Fe concentration and turbidity under different oxidation conditions using hydrophobic (PVDF) membrane as compared to sedimentation

pH	Conditions	Residual Fe (mg/L)	Residual turbidity (NTU)	Median diameter (μm)
7.5 (5 psi)	Sedimentation	3.24	3.79	0.62
	Microfiltration	0.45	0.00	0.75
8 (5 psi)	Sedimentation	1.81	0.97	0.86
	Microfiltration	0.10	0.00	1.30
7.5 (8 psi)	Sedimentation	3.49	3.94	0.65
	Microfiltration	0.44	0.00	1.10
8 (8 psi)	Sedimentation	1.94	1.06	0.86
	Microfiltration	0.11	0.00	3.51

Table 3
Various resistances under different pH, membrane type, and filtration pressure

pH	Filtration pressure, (psi)	R_m, (m^{-1})	R_f, (m^{-1})	R_c, (m^{-1})	R_t, (m^{-1})
Hydrophilic (mixed cellulose ester) membrane (0.48 m/s)					
7.5	5	4.30e10 (12.11%)	9.10e10 (25.63%)	2.21e11 (62.26%)	3.55e11 (100%)
	8	4.80e10 (5.44%)	1.87e11 (21.18%)	6.48e11 (73.38%)	8.83e11 (100%)
8	5	3.80e10 (7.50%)	8.90e10 (17.55%)	3.80e11 (74.95%)	5.07e11 (100%)
	8	4.00e10 (5.54%)	1.05e11 (14.54%)	5.77e11 (79.92%)	7.22e11 (100%)
Hydrophobic (PVDF) membrane (0.48 m/s)					
7.5	5	8.30e10 (24.41%)	6.90e10 (20.29%)	1.88e11 (55.30%)	3.40e11 (100%)
	8	8.60e10 (10.83%)	1.05e11 (13.22%)	6.03e11 (75.95%)	7.94e11 (100%)
8	5	8.50e10 (19.19%)	6.70e10 (15.12%)	2.91e11 (65.69%)	4.43e11 (100%)
	8	8.30e10 (13.17%)	1.03e11 (16.35%)	4.44e11 (70.48%)	6.30e11 (100%)

could be assumed constant since it was only important in the early stages of filtration.

Fig. 3(A) shows flux using hydrophobic (PVDF) membrane at three different filtration pressures under the laminar flow condition. The Reynolds number (N_{Re}) used in this study was 1,800. The initial flux was 955, 1,400, and 1,155 L/m^2h, respectively, at filtration pressures of 5, 8, and 10 psi. The steady flux was 280, 315, and 300 L/m^2h, respectively, at filtration pressures of 5, 8, and 10 psi. The initial and steady fluxes increased with filtration pressure. However, at a filtration pressure of 10 psi, values of initial and steady fluxes lower than those at 8 psi were obtained. Fig. 3(B) shows flux at three different filtration pressures under the turbulent flow condition. The Reynolds number (N_{Re}) used in this study was 3,400, and the initial flux was 1,290, 1,425, and 1,475 L/m^2h, respectively, at filtration pressures of 5, 8, and 10 psi. The steady flux was 310, 350, and 410 L/m^2h, respectively, at filtration pressures of 5, 8, and 10 psi. The initial and steady fluxes increased with the increase in filtration pressure. Iron removal efficiency of the microfiltration process was higher than that of the sedimentation process, as shown in Table 4. The Fe concentration in permeate was lower than the guide-

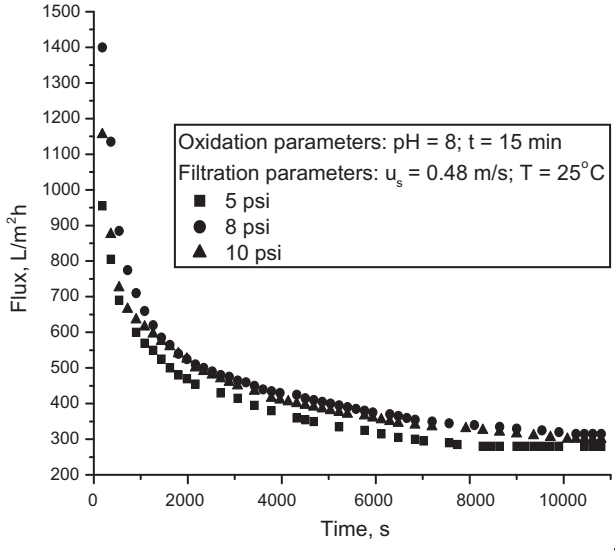

Fig. 3A. Flux at different filtration pressures in laminar region using hydrophobic (PVDF) membrane.

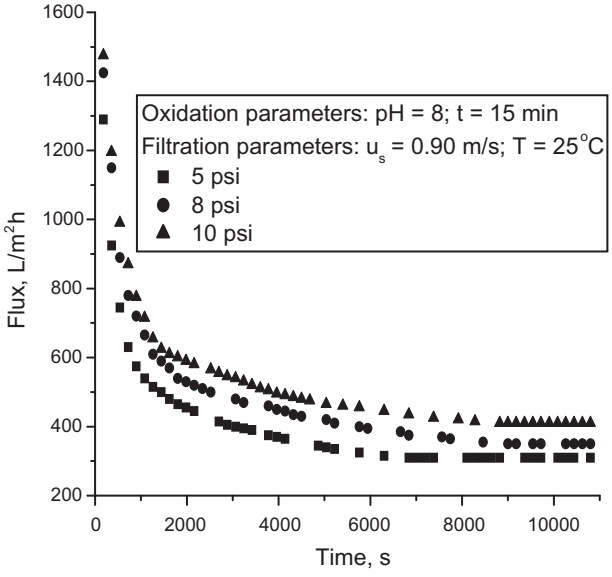

Fig. 3B. Flux at different filtration pressures in turbulent region using hydrophobic (PVDF) membrane.

line under all conditions. Turbidity in the permeate was all below detection limits and lower than that from sedimentation.

Table 5 summarizes various resistances as a function of filtration pressure and crossflow velocity under laminar and turbulent flow conditions. Cake resistance was the dominant one, which had the most significant effect on the decline in flux. Cake resistance increased with increasing filtration pressure. The increase in cake resistance with filtration pressure could be explained using average specific cake resistance and cake mass per unit filtration area analysis. The average specific cake resistance (α_{av}) and cake mass per unit filtration (w_c) increased with increasing filtration pressure. The average specific cake resistance is related to the compaction of the cakes, in which a cake with larger α has smaller voidage or porosity and causes better compaction. The higher value of average specific cake resistance and cake mass per unit filtration area under the laminar flow condition than that under the turbulent flow condition indicated a higher amount of and more compact cake was deposited on the membrane surface under the laminar flow condition. Average specific cake resistance and cake mass per unit filtration area increased with increasing filtration pressure because of cake compression and a higher amount of particles were retained by the membrane. The greater the specific cake resistance, the smaller was the filtration rate for a given pressure drop across the filter. Cake mass per unit filtration area increased with filtration pressure and decreased with increasing crossflow velocity [22].

3.3. Effects of manganese (Mn)

The effects of Mn on Fe removal were investigated in this study. During the oxidation process, Fe removal efficiency decreased with the increase in Mn concentration, while a higher Mn concentration resulted in higher Mn removal efficiency (Table 6). It might be due to the competition between Fe and Mn for oxygen. Wolthoorn et al. [30] found that the presence of Mn retarded the homogeneous and heterogeneous oxidation rates of Fe. Fe removal efficiency in the presence of Mn was above 90%, and less than 5% Mn was removed. Much higher Fe removal efficiency than Mn removal efficiency was related to the slow

Table 4
Residual Fe concentration ad turbidity under different conditions using hydrophobic (PVDF) membrane as compared to sedimentation

Crossflow velocity (m/s)	Filtration pressure (psi)	Conditions	Residual Fe (mg/L)	Residual turbidity (NTU)
0.48	5	Sedimentation	1.81	0.97
		Microfiltration	0.10	0.00
	8	Sedimentation	1.94	1.06
		Microfiltration	0.11	0.00-
	10	Sedimentation	1.74	0.88
		Microfiltration	0.09	0.00
0.90	5	Sedimentation	1.79	0.99
		Microfiltration	0.09	0.00
	8	Sedimentation	1.84	1.03
		Microfiltration	0.09	0.00
	10	Sedimentation	1.95	0.87
		Microfiltration	0.09	0.00

Table 5
Resistances under different filtration pressure and crossflow velocity using hydrophobic (PVDF) membrane

Crossflow velocity (m/s)	Filtration pressure (psi)	w_c, (kg/m^2)	α_{av}, (m/kg)	R_m, (m^{-1})	R_f, (m^{-1})	R_c, (m^{-1})	R_t, (m^{-1})
0.48	5	0.019	1.55e13	8.50e10 (19.19%)	6.70e10 (15.12%)	2.91e11 (65.69%)	4.43e11 (100%)
	8	0.023	1.91e13	8.30e10 (13.17%)	1.03e11 (16.35%)	4.44e11 (70.48%)	6.30e11 (100%)
	10	0.025	2.53e13	8.10e10 (9.79%)	1.07e11 (12.94%)	6.39e11 (77.27%)	8.27e11 (100%)
0.90	5	0.015	1.53e13	8.20e10 (20.50%)	8.50e10 (21.25%)	2.33e11 (58.25%)	4.00e11 (100%)
	8	0.021	1.80e13	8.40e10 (14.81%)	1.05e11 (18.52%)	3.78e11 (66.67%)	5.67e11 (100%)
	10	0.023	1.83e13	8.40e10 (13.88%)	1.10e11 (18.18%)	4.11e11 (67.94%)	6.05e11 (100%)
1.33	8	0.015	1.75e13	8.40e10 (18.63%)	1.00e11 (22.17%)	2.67e11 (59.20%)	4.51e11 (100%)

Table 6
Experimental results under various initial Mn concentrations

Initial concentration (mg/L)		Conditions	Residual concentration (mg/L)		Residual turbidity (NTU)
Fe	Mn		Fe	Mn	
75	0	Sedimentation	1.81	–	0.95
		Microfiltration	0.09	–	0.00
	2	Sedimentation	3.27	1.96	1.99
		Microfiltration	1.07	1.94	0.00
	5	Sedimentation	3.34	4.47	1.27
		Microfiltration	1.93	4.26	0.00
	7.5	Sedimentation	3.60	7.11	0.91
		Microfiltration	1.24	6.47	0.00
	37	Sedimentation	3.93	35.37	0.54
		Microfiltration	0.41	31.00	0.00

oxidation kinetics of Mn at circumneutral pH of air [11,33]. It was found that both Fe and Mn removal efficiencies increased after the microfiltration process. It could be concluded that in the microfiltration system, further oxidation process still continued. Davies and Morgan [6] found that Mn was more readily oxidized on surfaces than in solution. The solubility of contaminant metals could be lowered if they are adsorbed onto other precipitated metals [29]. Fe removal efficiency decreased with increasing initial Mn concentration when a low initial Mn concentration was used, and increased with increasing initial Mn concentration when a high initial Mn concentration was used.

Fig. 4 shows flux when using hydrophobic (PVDF) membrane under various initial Mn concentrations. The initial flux was 1,465, 760, 945, 1,095, and 1,415 L/m^{2}h, respectively, when the initial Mn concentration was 0, 2, 5, 7.5, and 37 mg/L. The steady flux was 440, 150, 205, 325, and 365 L/m^{2}h, respectively, when the initial Mn concentration was 0, 2, 5, 7.5, and 37 mg/L. The initial and steady fluxes obtained in the absence of Mn were higher than those in the presence of Mn. The initial and steady fluxes in the presence of Mn increased with increasing initial Mn concentration. It might be due to the larger particles at a higher initial Mn concentration, as shown in Fig. 5. The highest flux occurred when the initial Mn concentration was 37 mg/L. It was likely that the heterogeneous oxidation process was more significant than the homogenous oxidation process. The lowest flux and the smallest particle size occurred when the initial Mn concentration was 2 mg/L (Fig. 5). The particles with a small size had higher possibility of causing clogging on the membrane pore. Choo et al. [3] found that oxidized Mn had a more significant effect on membrane fouling than oxidized Fe. Yamamura et al. [32] found that the particle size of Fe was larger than that of Mn.

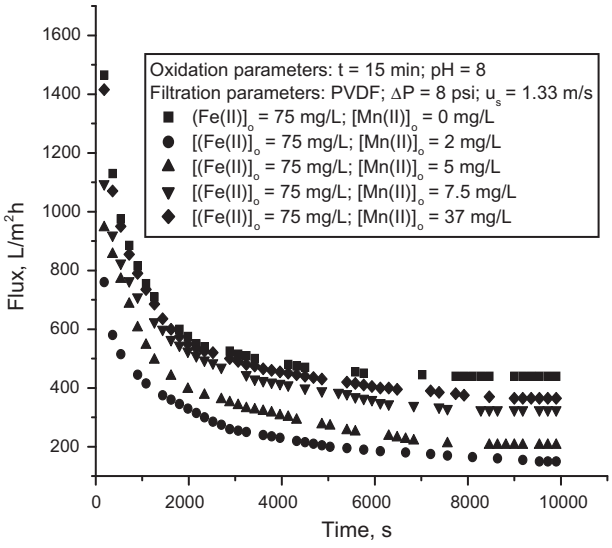

Fig. 4. Decline in flux as affected by various Mn(II) concentrations.

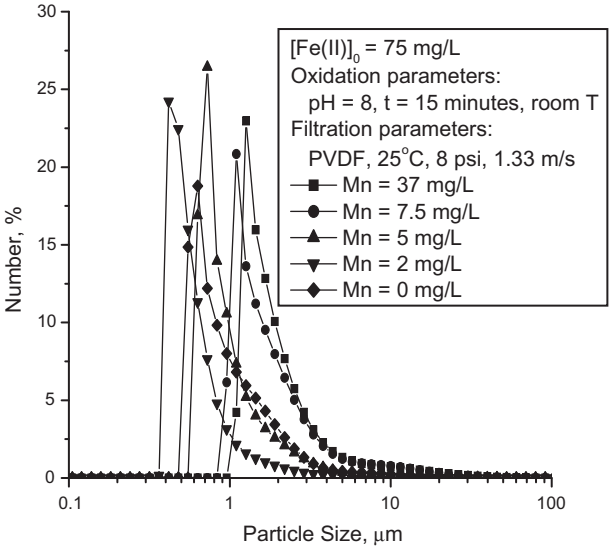

Fig. 5. Particle size distributions in the presence of Mn after oxidation process.

The particle size obtained after the microfiltration process was larger than those before microfiltration, owing to the further oxidation process on membrane surfaces.

3.4. Effects of HA

The effects of HA on Fe removal were investigated. Lower Fe removal efficiency in the presence of HA was found (Table 7). Fe removal efficiency decreased with increasing HA concentration, and it resulted in a higher concentration of Fe than the guideline, although the removal efficiency was still above 90%. The lower Fe removal efficiency in the presence of HA was because organic matter retarded the oxidation process [30]. HA removal efficiency increased with the increase in initial HA concentration. Charge neutralization and precipitation are the dominant mechanisms for HA removal at low pH. Adsorption (hydrophobicity and ligand exchange) is the dominant mechanism at high pH (pH > 7) [2,28]. Illes and Tombacz [18] found that at the same pH, the adsorption capacity of magnetite would increase with increasing HA in solution. Adsorption phenomena involve the exchange of hydroxyl groups of iron oxide by the adsorbing ligands [4]. HA removal efficiency was very high, which might be because of the usage of high Fe concentrations in this study and removal of HA by co-precipitation. In addition, high initial Fe concentrations resulted in large amounts of iron oxides. Large amounts of iron oxides formed in this system provided more surface area for organic matter to be adsorbed.

Fig. 6 shows flux under various initial HA concentrations. The initial flux was 1,465, 1,300, 1,135, and 865 L/m²h, respectively, when the initial HA concentration was 0, 4, 12, and 30 mg/L. The steady flux was 440, 365, 245, and 170 L/m²h, respectively, when the initial HA concentration was 0, 4, 12, and 30 mg/L The lower value of the initial and steady fluxes was obtained in the presence of HA. The fluxes decreased with increasing HA concentration. It might be because

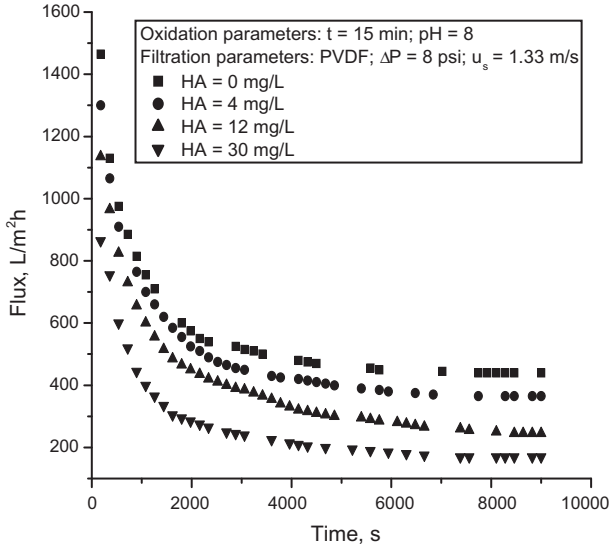

Fig. 6. Decline in flux as affected by various concentrations of HA.

Table 7
Experimental results under various initial HA concentrations

Initial concentration (mg/L)		Conditions	Residual concentration (mg/L)	
Fe	HA		Fe	HA
75	0	Sedimentation	1.81	–
		Microfiltration	0.09	–
	4	Sedimentation	3.65	3.14
		Microfiltration	2.44	1.46
	12	Sedimentation	4.91	2.99
		Microfiltration	2.99	1.35
	30	Sedimentation	8.32	3.06
		Microfiltration	3.37	2.53

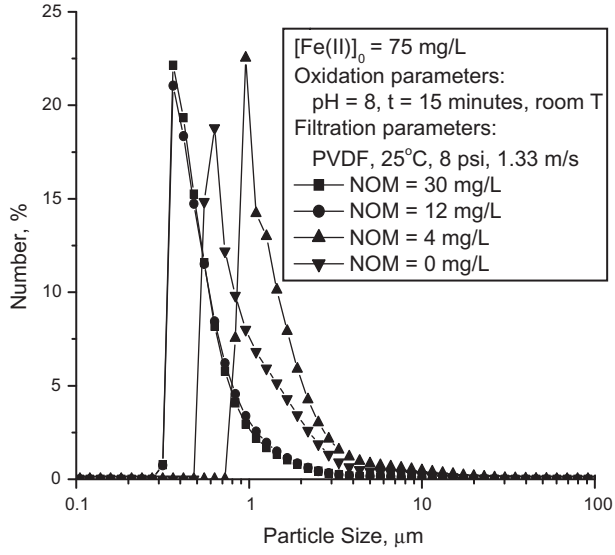

Fig. 7. Particle size distributions in the presence of HA after oxidation process.

of the hydrophobic interaction between particles and membrane. The membrane type used in this study was hydrophobic in nature. The particle surface changed from hydrophilic to hydrophobic in the presence of organic matter [4,9]. The hydrophobicity of particles also explains the increase in HA removal at higher initial HA concentrations. Schafer et al. [27] found that the flux decreases much faster when a higher HA concentration was used.

Table 7 shows that the Fe concentration in permeate was above the guideline in the presence of HA. The surface charge of the particles obtained after the oxidation process became more negative in the presence of HA. Particles had negative charge when covered with adsorbed HA, showing that ligand exchange was more dominant than electrostatic interaction between iron oxide surfaces and HA [19]. The particle size decreased with increasing HA, as shown in Fig. 7 because of the more negative surface charge of the particles, which caused the repulsion interaction between the particles and prevented the aggregation [18]. It is proposed that cake resistance contributed the most to the decline in flux. However, at high initial HA concentrations, the effect of fouling resistance could not be neglected because of the smaller particles at high initial HA concentrations. The higher cake resistance with increasing initial HA concentration was because of the higher average cake specific resistance and cake mass per unit filtration area. Average specific cake resistance and cake mass per unit filtration area were higher in the presence of HA.

4. Conclusions

Iron removal under various conditions of oxidation-microfiltration membrane processes was investigated in this study. From the experimental results, the following conclusions are made:

(1) The higher pH and the longer oxidation time gave higher Fe removal efficiency.
(2) The microfiltration process enhanced iron removal.
(3) Various conditions in the microfiltration system, such as membrane types, filtration pressure, and crossflow velocity, had significant effects on permeate flux and insignificant effects on Fe removal efficiency.
(4) Hydrophilic and hydrophobic membranes gave similar trends in results, except differences in permeate flux.
(5) Permeate flux generally increased with filtration pressure, either under the laminar or turbulent flow condition.

(6) Increase in crossflow velocity resulted in increasing permeate flux.
(7) Cake resistance contributed more than other resistances in terms of decline in flux under all microfiltration conditions.
(8) The presence of Mn and HA reduced Fe removal efficiency and permeate flux.

Acknowledgement

Lanny Setyadhi would like to acknowledge the full international scholarship awarded by the National Taiwan University of Science and Technology during her master's degree.

References

[1] B.Y. Cho, Iron removal using an aerated granular filter, Process Biochem. 40(10) (2005) 3314–3320.
[2] K.H. Choo, S.K. Kang, Removal of residual organic matter from secondary effluent by iron oxides adsorption, Desalination 154(2) (2003) 139–146.
[3] K.H. Choo, H. Lee, S.J. Choi, Iron and manganese removal and membrane fouling during UF in conjunction with prechlorination for drinking water treatment, J. Membr. Sci. 267 (1–2) (2005) 18–26.
[4] R.M. Cornell, U. Schwertmann, The Iron Oxides: Structure, Properties, Reactions, Occurrences, and Uses, 2nd ed, Wiley-VCH, Weinheim, 2003.
[5] B. Das, P. Hazarika, G. Saikia, H. kalita, D. C. Goswami, H. B. Das, S. N. Dube, R. K. Dutta, Removal of iron from groundwater by ash: A systematic study of a traditional method, J. Hazard. Mater. 141(3) (2007) 834–841.
[6] S.H.R. Davies, J.J. Morgan, Manganese(II) oxidation kinetics on metal oxide surfaces, J. Colloid Interface Sci. 129(1) (1989) 63–77.
[7] D. Ellis, C. Bouchard, G. Lantagne, Removal of iron and manganese from groundwater by oxidation and microfiltration, Desalination 130(3) (2000) 255–264.
[8] European Communities (EC) Drinking Water No. 2 Regulations 2007, S.I. No. 278 of 2007.
[9] H. Fu, X. Quan, Complexes of fulvic acid on the surface of hematite, goethite, and akaganeite: FTIR observation, Chemosphere 63(3) (2006) 403–410.
[10] M. Gotic, S. Music, Mossbauer, FT-IR and FE SEM investigation of iron oxides precipitated from $FeSO_4$ solutions, J. Mol. Struct. 834–836 (2007) 445–453.
[11] K.B. Hallberg, D.B. Johnson, Biological manganese removal from acid mine drainage in constructed wetlands and prototype bioreactors, Sci. Total Environ. 338(1–2) (2005) 115–124.
[12] M. Hassellov, K.O. Buesseler, S.M. Pike, M. Dai, Application of crossflow ultrafiltration for the determination of colloidal abundances in suboxic ferrous-rich groundwaters, Sci. Total Environ. 372(2–3) (2007) 636–644.
[13] M. Hove, R.P. van Hille, A.E. Lewis, Iron solids formed from oxidation precipitation of ferrous sulfate solutions, AIChE J. 53(10) (2007) 2569–2577.
[14] M.T. Hung, J.C. Liu, Reclamation of backwash water by crossflow microfiltration—a case study, J. Water Supply: Res. Technol.-AQUA 56(8) (2007) 8479–8493.
[15] K.J. Hwang, Y.L. Hsu, K.L. Tung, Effect of particle size on the performance of crossflow microfiltration, Adv. Powder Technol. 17(2) (2006) 189–206.
[16] K.J. Hwang, H.C. Hwang, The purification of protein crossflow microfiltration of microbe/protein mixtures, Sep. Purif. Technol. 51(3) (2006) 416–423.
[17] K.J. Hwang, C.Y. Liao, K.L. Tung, Analysis of particle fouling during microfiltration by use of blocking models, J. Membr. Sci. 287(2) (2007) 287–293.
[18] E. Illes, E. Tombacz, The effect of humic acid adsorption on pH-dependent surface charging and aggregation of magnetite nanoparticles, J. Colloid Interface Sci. 295(1) (2006) 115–123.
[19] G.V. Korshin, M.M. Benjamin, R.S. Sletten, Adsorption of natural organic matter (NOM) on iron oxide: Effects on NOM composition and formation of organo-halide compounds during chlorination, Water Res. 31(7) (1997) 1643–1650.
[20] E.K. Lee, V. Chen, A.G. Fane, Natural organic matter (NOM) fouling in low pressure membrane filtration—effect of membranes and operation modes, Desalination 218(1–3) (2008) 257–270.
[21] D. Li, J. Zhang, H. Wang, H. Yang, B. Wang, Operational performance of biological treatment plant for iron and manganese removal, J. Water Supply: Water Res.-AQUA 54(1) (2005) 15–24.
[22] A.A. McCarthy, P.K. Walsh, G. Foley, Experimental techniques for quantifying the cake mass, the cake and membrane resistances and the specific cake resistance during crossflow filtration of microbial suspension, J. Membr. Sci. 201(1) (2002) 31–45.
[23] S.C. Pang, S.F. Chin, M.A. Anderson, Redox equilibria of iron oxides in aqueous-based magnetite dispersions: Effect of pH and redox potential, J. Colloid Interface Sci. 311(1) (2007) 94–101.
[24] H.D. Pedersen, D. Postma, R. Jakobsen, O. Larsen, Fast transformation of iron oxyhydroxides by the catalytic action of aqueous Fe(II), Geochim. Cosmochim. Acta 69(16) (2005) 3967–3977.
[25] P. Roccaro, C. Barone, G. Mancini, F.G.A. Vagliasindi, Removal of manganese from water supplies intended for human consumption: A case study, Desalination 210(1–3) (2007) 205–214.
[26] J. Sallanko, E. Lakso, J. Ropelinen, Iron behavior in the ozonation and filtration of groundwater, Ozone Sci. Eng. 28(4) (2006) 369–273.
[27] A.I. Schafer, U. Schwicker, M.M. Fischer, A.G. Fane, T.D. Waite, Microfiltration of colloids and natural organic matter, J. Membr. Sci. 171(2) (2000) 151–172.
[28] J.M. Sieliechi, B.S. Lartiges, G.J. Kayem, S. Hupont, C. Frochot, J. Thieme, J. Ghanbaja, J.B. d'Espinose de la Caillerie, O. Barres, R. Kamga, P. Levitz, L.J. Michot, Changes in humic acid conformation during coagulation with ferric chloride: Implications for drinking water treatment, Water Res. 42(8–9) (2008) 2111–2123.
[29] L.E. Voges, P.E. Benjamin, M.M. Chang, Use of iron oxides to enhance metal removal in crossflow microfiltration, J. Environ. Eng. 127(5) (2001) 411–419.
[30] A. Wolthoorn, E.J.M. Temminghoff, L. Weng, W.H. van Riemsdijk, Colloid formation in groundwater: Effect of phosphate, manganese, silicate and dissolved organic matter on the dynamic heterogeneous oxidation of ferrous iron, Appl. Geochem. 19(4) (2004) 611–622.
[31] World Health Organization, Guidelines for Drinking Water Quality, third ed., vol. 1, WHO, Geneva, 2006.
[32] H. Yamamura, S. Chae, K. Kimura, Y. Watanabe, Transition in fouling mechanism in microfiltration of a surface water, Water Res. 41(17) (2007) 3812–3822.
[33] J. Zhang, L.W. Lion, Y.M. Nelson, M.L. Shuler, W.C. Ghiorse, Kinetics of Mn(II) oxidation by *Leptothrix discophora* SS1, Geochimica Cosmoshimica 66(5) (2002) 773–781.